Grey Swan Tropical Cyclones

Ning Lin[1*] and Kerry Emanuel[2]

[1]Department of Civil and Environmental Engineering, Princeton University, Princeton, NJ 08544, USA

[2]Department of Earth, Atmospheric, and Planetary Sciences, Massachusetts Institute of Technology, Cambridge, MA 02139-4307, USA

[*]Corresponding author, nlin@princeton.edu

Abstract

We define “Grey swan” tropical cyclones as high-impact storms that would not be predicted based on history but may be foreseeable using physical knowledge together with historical data. Here we apply a climatological-hydrodynamic method to estimate grey swan TC storm surge threat for three highly vulnerable coastal regions. We identify a potentially large risk in the Persian Gulf, where TCs have never been recorded, and larger-than-expected threats in Cairns, Australia, and Tampa, Florida. Grey swan TCs striking Tampa, Cairns, and Dubai can generate storm surges of about 6 m, 5.7 m, and 4 m, respectively, with estimated annual exceedance probabilities of about 1/10000. With climate change, these probabilities can increase significantly over the 21st century (to 1/3100-1/1100 in the middle and 1/2500-1/700 towards the end of the century for Tampa). Worse grey swan TCs, inducing surges exceeding 7 m in Dubai and 11 m in Tampa, are also revealed with non-negligible probabilities, especially towards the end of the century.

Introduction

The term "Black swans"[1,2] is a metaphor for high-consequence events that come as a surprise. Some high-consequence events that are unobserved and unanticipated may nevertheless be predictable (though perhaps with large uncertainty). Such to-some-extent-predictable, low-probability, high-impact events may be referred to as "grey swans"[3,4] (or, sometimes, "perfect storms"[5]). Unlike truly unpredicted and unavoidable black swans, which can be dealt with only by fast reaction and recovery, grey swans-although also novel and outside experience-can be better foreseen and systematically prepared for[4,5].

Tropical cyclones (TCs) often produce extreme wind, rainfall, and storm surges in coastal areas. Storm surges are especially complex functions of TC characteristics (track, intensity, and size) and coastal features (geometry and bathymetry), and they are also the most fatal and destructive aspect of TCs (see ref 6 for a comprehensive review of global TC surge observations and impacts). Hence, storm surge is an appropriate and practical metric for identifying grey swan TCs. The most infamous TC disasters early in this century were attributable to storm surges, but they should not be considered grey swans, as they had been or could have been anticipated based on historical observations and/or experience. Hurricane Katrina (2005), the costliest U.S. natural disaster, generated the highest U.S recorded surge inundation (~10 m)[7], but its impact on New Orleans, due largely to the levee failure, had been anticipated by various studies[8]. Cyclone Nargis (2008), the worst natural disaster in Myanmar's history and one of the deadliest TCs worldwide, struck Myanmar's Ayeyarwady River Delta at an unusually low latitude (near 16° N) and induced extreme surges (over 5 m); however, the catastrophic fatalities in the hardest-hit areas were largely due to the lack of evacuation plans and cyclone awareness[9], although intense tropical cyclones had been active in the Bay of Bengal and

made landfall in Myanmar (e.g., in 2006). Hurricane Sandy, which devastated the U.S. Northeast coast in 2012, set the record-high storm tide (3.4 m) at the Battery in New York City (NYC); however, its storm surge (2.8 m) at the Battery was much lower than those of the 1821 NY hurricane (4.0 m)[10,11] and more severe grey swan TCs (4.5-5 m) that had been simulated for the region[12,13]. Typhoon Haiyan (2013), the deadliest TC in Philippine history and probably the most powerful TC to make landfall worldwide, generated extreme water levels up to 8 m near the most affected Tacloban area[14], but the water level was comparable to those induced by earlier storms, including a similarly severe typhoon that struck the area in 1897 (7.3 m)[15].

Prediction of a grey swan TC, by definition, is meaningful and practically useful only when associated with some likelihood/probabilistic statement, e.g., the probability of exceeding the storm surge level induced by the TC in a year is 10^{-3}. The Monte Carlo (MC) method, based on numerous synthetic simulations, is an important way to assess the probability of grey swan TCs. Most current MC methods[16,17,18] simulate synthetic TCs using (quite limited) historical TC statistics. In contrast, a statistical-deterministic model[19], which is independent of the TC record, simulates TC environments statistically and generates TCs in the simulated environments deterministically. This statistical-deterministic approach may sometimes be more reliable, as observations of the large-scale TC environment are often better constrained than those of TC characteristics in areas with very limited TC history. It is also more likely to generate unexpected but realistic grey swan TCs, because, rather than extrapolating historical TCs, it applies physical knowledge of TCs and ample observations of the large-scale environment. Moreover, as the synthetic TC environments can be generated for any given climate state, this model can simulate grey swan TCs not only in the current and past climates but also in projected future climates[20]. As TC activity may vary with changing climate[21,22,23,24], the model enables quantitative projection

of how grey swan TCs will evolve in the future. This statistical-deterministic TC model has been integrated with hydrodynamic surge models[25] into a climatological-hydrodynamic method[13], which has been shown to generate extreme storm surges that are far beyond historical records but are compatible with geological evidence[26]. The method has been used to study storm surge risk and mitigation strategies for NYC[27,28], and it is applicable to any coastal city. Here we apply the method to another three highly vulnerable regions: Tampa in Florida, Cairns in Australia, and the Persian Gulf; we identify their grey swan TCs as the synthetic TCs that are associated with extremely low annual exceedance probabilities (large mean return periods) of the induced storm surges (see Methods).

Tampa

Tampa, located on the central west Florida coast, is highly susceptible to storm surges. Although many fewer storms have made landfall in this area than in regions farther north and west on the Gulf Coast or further south on the Florida Coast, Tampa Bay is surrounded by shallow water and low-lying lands; a 6-m rise of water can inundate much of the Bay's surroundings[29]. Two significant historical events have affected Tampa. The Tampa Bay hurricane of 1848 produced the highest storm tide ever experienced in the Bay, about 4.6 m, destroying many of the few human works and habitations then in the area. The Tampa Bay hurricane of 1921 produced an estimated storm tide of 3-3.5 m, inducing severe damage (10 million in 1921 USD).

To investigate the current TC threat for Tampa, we simulate 7800 Tampa Bay synthetic TC surge events in the observed climate of 1980-2005 as estimated from the NCEP/NCAR reanalysis[30]. To study how the threat will evolve from the current to future climates, we apply

each of 6 climate models to simulate 2100 surge events for the climate of 1980-2005 (control) and 3100 surge events for each of the three climates--2006-2036 (early 21st century), 2037-2067 (middle), and 2068-2098 (late)--under the IPCC AR5 RCP8.5 emission scenario. The 6 climate models, selected as in ref 24 from CMIP5 (Coupled Model Intercomparison Project Phase 5), are CCMS (CCMS4; NCAR), GFDL (GFDL-CM3; NOAA), HADGEM (HADGEM2-ES; UK Met Office Hadley Center), MPI (MPI-ESM-MR; Max Planck Institution), MIROC (MIROC5; CCSR/NIES/FRCGC, Japan), and MRI (MRI-CGCM3; Meteorological Research Institute, Japan).

The large synthetic surge database includes many extreme events affecting Tampa. As a comparison, the 1921 Tampa surge event is also simulated (Fig. 1a). The 1921 Tampa hurricane had a track similar to that of the 1848 Tampa hurricane[31], traveling northwestward over the Gulf of Mexico and making landfall north of Tampa Bay. The "worst" synthetic case (among 7800 events) in the reanalysis climate of 1980-2005 has a similar track (Fig. 1b). However, this grey swan TC is more intense (upper Cat 3, compared to the lower Cat-2 1921 storm), inducing a higher surge at Tampa of 5.9 m (compared to 4.0 m simulated for the 1921 storm). We have also identified grey swan TCs affecting Tampa that have very different tracks, especially those moving northward parallel to the west Florida coast before making landfall. For example, Fig. 1(c) shows an extremely intense storm (104 m/s; "worst" case generated under the late 21st century climate projected by HADGEM) that moves northward parallel to the coast and turns sharply towards Tampa Bay, inducing a storm surge of 11.1 m in Tampa. In such cases, the storm surges are likely amplified by coastally trapped Kevin Waves. These waves form when the storm travels along the west Florida coast and propagate northward along the Florida shelf, enhancing the coastal surges, especially when the storm moves parallel to the shelf and at

123 comparable speed to the wave phase speed[32]. This geophysical feature makes Tampa Bay even
124 more susceptible to storm surge.

125 These grey swan TCs have very low probabilities, which can be quantified only within
126 the full spectrum of events. Fig. 2 shows the estimated storm surge level for Tampa as a function
127 of (mean) return period for the reanalysis climate of 1980-2005. The grey swan surge of 5.9 m
128 (Fig. 1b) has a return period of over 10,000 years in the 1980-2005 climate. In comparison, the
129 1000-year surge is about 4.6 m and the 100-yr surge is about 3.2 m. The surge level of the 1921
130 storm (approximately 3.3-3.8 m, as it likely happened at low tide) has an estimated return period
131 of 100-300 years in the 1980-2005 climate. We note here a potentially large uncertainty in the
132 analysis. In the simulations, we take the storm outer radius R_o to be its statistical mean[33] to
133 generate the radius of the maximum wind R_m (see Methods). As shown previously[26], neglecting
134 the statistical variation of storm size may greatly underestimate the surge risk, as the
135 distributions of the size metrics (R_o and R_m) may be positively skewed[33]. Indeed, a sensitivity
136 analysis for Tampa shows that the estimated surge return periods would be significantly reduced
137 if a lognormal distribution of R_o [33] (with the same mean) was applied; for example, the return
138 period of the 1921 storm surge could be reduced to as little as 60 years (not shown). However,
139 the result is very sensitive to the specific distribution of R_o, which itself is largely uncertain due
140 to data limitations and lack of fundamental knowledge of what controls the TC size in nature[34,35].
141
142 The more severe grey swan surges of above 8 m up to 11 m (Fig 1c) have extremely low
143 or negligible probabilities in the 1980-2005 climate, but they are projected to happen as 5,000-
144 150,000-yr events in the late 21st century. As shown in Fig. 3, the 6 climate models project that
145 the return period of the storm surges for Tampa will significantly decrease over the 21st century,

146 especially for the extremes (grey swans). This increase in storm surge threat is mainly due to the
147 increase in storm frequency and intensity. The magnitude of the surge, especially for the
148 extremes, is projected to increase by all 6 models, and the CCSM, HADGEM, and MPI models
149 project relatively larger increases (see Supplemental Fig. S1). The overall frequency of the
150 Tampa Bay storms is also projected to increase moderately (<25%) according to the CCSM,
151 HADGEM, and MRI models; greatly (<75%) according to MIROC and MPI; or extremely
152 (240%) according to GFDL (noted in Fig. 3). As a result, the CCSM and HADGEM models
153 project the largest increase in the frequency of the grey swans and little change in the normal
154 events while GFDL projects a relatively uniform increase in the frequency of all events, and the
155 other three models project relatively large (small) increases in the frequency of extremes (normal
156 events). Hence, large uncertainties exist among the climate models in the probable increase of
157 grey swans over the century. For example, a ten-thousand-year event in the late 20th century will
158 become a 1.5-7, 1.1-3.1, and 0.7-2.5 thousand-year event in the early, middle, and late 21st
159 century, respectively, depending on the climate models; and a one-thousand-year event in the
160 late 20th century will become a 2.7-13, 1.1-5.3, and 0.6-4.5 hundred-year event in the early,
161 middle, and late 21st century, respectively. (Supplementary Fig. S2 (S3) illustrates, for various
162 levels of events, how the return periods (annual exceedance probabilities) decreases (increases)
163 over the 21st century, projected by each of the 6 climate models.) Here the effect of neglecting
164 the variability of storm size may be relatively small for the projections of the change of the
165 probability. However, this analysis neglects the possible increase of the magnitude of storm size
166 in a warmer climate. Although such an increase in storm size, as suggested by potential intensity
167 theory[36], would further increase the surge risk[13], the effect of climate change on storm size has
168 yet to be investigated observationally and numerically.

Cairns

The TC threat to Cairns, in the far north of Queensland, may not be well recognized. The city is located about 300 km south of Bathurst Bay, which was hit in 1899 by Cyclone Mahina (the most intense TC in the Southern Hemisphere, inducing what may have been the highest surge inundation (13 m) in the historical record[37]). According to the Australian Bureau of Meteorology, at least 53 cyclones have affected Cairns since it was founded in 1876, and several high-intensity storms (e.g., Cyclones Larry in 2006 and Yasi in 2011) were near-misses. Recent events include Cyclones Justin in 1997, Rona in 1999, and Steve in 2000, all making landfall north of Cairns; although these storms (< Cat 2) generated storm surges in Cairns of less than 1 m, they induced major flooding (due also to tide and waves) and significant damage ($100-190 million) in the area. (Simulations of these historical cyclones, in comparison with observations, are shown in Supplementary Fig. S4.)

To study the TC threat for Cairns, we simulate 2400 synthetic Cairns TC surge events in the NCEP/NCAR reanalysis climate of 1980-2010. The "worst" surge for Cairns is about 5.7 m, induced by an intense storm (80 m/s) traveling perpendicularly to the coast and landfalling just north of Cairns (Fig. 4a). This grey swan TC is much stronger than Cyclones Justin, Rona, and Steve and makes landfall much closer to Cairns. It resembles a hypothetical Cyclone Yasi that is moderately intensified (by about 10 m/s) and shifted northward by about 160 km.

As shown by the estimated surge return curve in Fig. 4b, the grey swan surge of 5.7 m has a return period of over 10,000 years in the 1980-2010 climate. As a reference, the 1000-year surge is about 3.5 m, and the 100-yr surge is about 1.6 m. These results are significantly higher

than previous estimates based on synthetic storm databases generated by statistically extending the historical storm records. For example, one such study[38] estimated that the 1000-yr storm surge level for Cairns is about 2.3 m (storm tide of 2.9 m) and the 100-yr surge level is about 1.3 m (storm tide of 2.0 m); another[39] estimated the 10,000-yr storm tide to be 2.6 m, the 1,000-yr storm tide to be 2.2 m, and the100-yr storm tide to be 1.8 m. The lower estimates in these previous analyses, especially for the most extreme events, were deduced by extrapolating the storm record from several decades to tens of thousands of years. Analyses based on geological evidence of paleo coastal inundations also yielded much higher estimates of such extremes for the north Queensland coast than these historical-storm-based estimates[40]; our results are more consistent with the geological evidence (Nott, personal communication).

The Persian Gulf

The Persian Gulf is a Mediterranean Sea of the Indian Ocean, connected to the Arabian Sea through the Strait of Hormuz and Gulf of Oman. The Persian Gulf is comprised of hot, shallow, and highly saline water, which can support the development of intense TCs and storm surges. However, no TC has been observed in the Persian Gulf, and TC development in the Arabian Sea is limited by the region's typically low humidity and high wind shear[41]. Cyclone Gonu (2007), the strongest historical TC in the Arabian Sea (Cat 3; 78 fatalities and 4.4 billion in damage), came close to entering the Persian Gulf, making landfall at the month of the Gulf on the easternmost tip of Oman and then in southern Iran. It is scientifically interesting and socially important to ask if such a strong TC can travel into the Persian Gulf.

To answer this question, we assess the TC threat for three major cities bordering the Persian Gulf: Dubai, Abu Dhabi, and Doha. For each of these cities, we simulate 3100 synthetic TC surge events in the NCEP/NCAR reanalysis climate of 1980-2010. Since the maximum width of the Persian Gulf is only about 340 km, it may be poorly resolved by the NCAR/NCEP reanalysis resolution of 2.5 degrees (about 250 km); thus we also apply a higher-resolution reanalysis dataset, the NASA' Modern-Era Retrospective Analysis[42] (MERRA; with resolution of 0.67 degrees x 0.5 degrees), to simulate TC surge events in Dubai. The obtained surge levels and probabilities, however, are very similar for the two datasets. We here present the result for Dubai from the MERRA reanalysis (while the results for Dubai, Abu Dhabi, and Doha from the NCEP/NCAR reanalysis are shown in the Supplement). Some of the synthetic storms originate in the Arabian Sea and move into the Persian Gulf, but the majority originates, surprisingly, within the Gulf. Moreover, the most extreme surges are all induced by intense storms that originate within the Gulf.

Fig. 5a shows the "worst" surge (among 3100 events in the climate of 1980-2010) for Dubai. This grey swan TC originates in the northwest region of the Persian Gulf, moves southeastwards in the Gulf, and makes landfall north of Dubai with extremely high intensity (115 m/s), generating a storm surge of 7.4 m in Dubai. The intensity of this grey swan TC is far beyond the highest observed TC intensity worldwide (Typhoon Haiyan of 87 m/s). This extremely high wind intensity is owing to very large potential intensities (PIs), made possible by high sea surface temperature (SST; with summertime peak values in the range of 32-35ºC[43]) and the deep dry adiabatic temperature profiles characteristic of desert regions. Indeed, the PI calculated using the Dammam (Saudi Arabia) atmospheric sounding and an SST of 32-35ºC is between 109 m/s and 132 m/s. (The daily PI calculated using this sounding and the Hadley

Center observed SST, shown in Supplementary Fig. S5, confirms this result). Furthermore, surface cooling from deep-water upwelling is nearly impossible in this shallow[1], highly saline, and mixed body of water, and when, occasionally, the wind shear is small, the storm can fully achieve its potential intensity. (We note, however, that the estimated pressure intensity has not been similarly evaluated, which will be done in the future, but the storm surge is less sensitive to the pressure than to the wind intensity.)

Fig. 5b shows the second highest synthetic surge generated for Dubai. This grey swan TC originates in the southeast region of the Persian Gulf, moves directly towards the coast, and makes landfall almost perpendicular to the coast and just north of Dubai, generating a storm surge of 5.7 m in Dubai. The storm intensity is moderate (65 m/s). It is not necessary for the storm to be extremely intense in order to generate extreme surges; some near "perfect" combination of track, intensity, and size can induce devastating surge inundation in Dubai, given its unusual shallow-water surroundings.

Nevertheless, given the prohibiting atmospheric environment in the region, these extreme grey swan TCs have very low probabilities, with return periods on the order of 30,000-200,000 years (Fig. 5c). Also, the surge level decreases rapidly with decreasing return period. The 10^4-year surge for Dubai is about 4 m and the 10^3-yr surge is about 1.9 m. The surges for return periods less than 100 years are very small. Similar and even higher surge levels for Abu Dhabi and Doha are also estimated using the NCAR/NCEP reanalysis (see Supplementary Figs. S6 and S7).

[1] The mean depth of the Persian Gulf is 36 m, with a maximum depth of 90 m.

We note that these analyses are based on the climate of 1980-2010, during which the Arabian Sea's synthetic TC activity increased, likely due to a decrease in the wind shear[44]. Thus, although TC development is limited in the Persian Gulf, a large TC threat exists and may be very sensitive to changes of the atmospheric circulation in the region. Moreover, the SST in the Persian Gulf had an upward significant trend during the period of 1950-2010, with an abrupt increase in the 1990-2010 era[43]. Further warming of the ocean may further increase the chance of the Persian Gulf region being struck by an extreme storm.

Final Remarks

Assessments of the risks associated with natural hazards such as tropical cyclones have been limited by the comparatively short length of historical records. This limitation is being overcome by the new field of paleotempestology, which identifies TC events in the geological record, and by bringing knowledge of storm physics to bear on the problem. Here we have used a physically-based climatological-hydrodynamic method to assess the likelihood of highly destructive events for three regions. Uncertainty in storm size induces uncertainty in the estimated probabilities; accounting for the variation of storm size from storm to storm and in different climates, when more reliable information on which becomes available, may yield significantly higher estimated TC threats. In addition to the storm surge that we focus on here, coastal inundation is also affected by the astronomical tide, waves, sea level rise, and future shoreline changes[45], all of which will amplify the impact of grey swan tropical cyclones.

References

[1] Taleb, N. N. *The Black Swan: The Impact of the Highly Improbable Fragility*. Random House LLC (2010).

[2] Aven, T. On the meaning of a black swan in a risk context. *Safety science*, 57, 44-51 (2013).

[3] Nafday, A. M. Strategies for Managing the Consequences of Black Swan Events. *Leadership and Management in Engineering*, 9(4), 191-197 (2009).

[4] Stein, J. L. & Stein, S. Gray swans: comparison of natural and financial hazard assessment and mitigation. Nat Hazards 72, 1279–1297 (2014).

[5] Paté Cornell, E. On "Black Swans" and "Perfect Storms": Risk Analysis and Management When Statistics Are Not Enough. *Risk Analysis* 32, 1823–1833 (2012).

[6] Needham, H., Keim, B. D. & Sathiaraj, D. A Review of Tropical Cyclone-Generated Storm Surges: Global Data Sources, Observations and Impacts. *Reviews of Geophysics*. (2015). doi:10.1002/2014RG000477

[7] Fritz, H. M. et al. Hurricane Katrina storm surge distribution and field observations on the Mississippi Barrier Islands. *Estuarine, Coastal and Shelf Science* 74, 12–20 (2007).

[8] SA, A. Scientists' fears come true as hurricane floods New Orleans. (2005).

[9] Fritz, H. M., Blount, C. D., Thwin, S., Thu, M. K. & Chan, N. Cyclone Nargis storm surge in Myanmar. *Nature Geoscience* 2, 448–449 (2009).

[10] Scileppi, E. & Donnelly, J. P. Sedimentary evidence of hurricane strikes in western Long Island, New York. *Geochem. Geophys. Geosyst.* 8, Q06011 (2007).

[11] Brandon, C. M., Woodruff, J. D., Donnelly, J. P. & Sullivan, R. M. How Unique was Hurricane Sandy? Sedimentary Reconstructions of Extreme Flooding from New York Harbor. *Scientific Reports* 4, 7366 (2014).

[12] Lin, N., K. A. Emanuel, J. A. Smith, and E. Vanmarcke (2010), Risk assessment of hurricane storm surge for New York City, *J. Geophys. Res.*, 115, D18121, doi:10.1029/2009JD013630.

[13] Lin, N., Emanuel, K., Oppenheimer, M. & Vanmarcke, E. Physically based assessment of hurricane surge threat under climate change. *Nature Climate Change* 2, 1–6 (2012).

[14] Mas, E., J. Bricker, S. Kure, B. Adriano, C. Yi, A. Suppasri, and S. Koshimura, Field survey report and satellite image interpretation of the 2013 Super Typhoon Haiyan in the Philippines, *Natural Hazards Earth System Science*, 15, 817-825, (2015).

[15] Bankoff, G. (2003), Cultures of Disaster: Society and Natural Hazard in the Philippines, Published by RoutledgeCurzon, London, United Kingdom, 232 pp.

[16] Vickery, P., P. Skerlj, and L. Twisdale. Simulation of hurricane risk in the U.S using empirical track model, *J. Struct. Eng.*, 126(10), 1222–1237, (2010).

[17] Toro, G. R., D. T. Resio, D. Divoky, A. W. Niedoroda, and C. Reed. Efficient joint-probability methods for hurricane surge frequency analysis, *Ocean Eng.*, 37(1), 125–134, (2010).

[18] Hall, T. M., & Sobel, A. H. On the impact angle of Hurricane Sandy's New Jersey landfall. *Geophysical Research Letters*, 40(10), 2312-2315, (2013).

[19] Emanuel, K., Ravela, S., Vivant, E. & Risi, C. A Statistical deterministic approach to hurricane risk assessment. *Bull. Amer. Meteor. Soc.,* 87, 299-314 (2006).

[20] Emanuel, K., Sundararajan, R. & Williams, J. Hurricanes and global warming: results from downscaling IPCC AR4 simulations. *Bull. Am. Meteor. Soc.*, 89, 347–367 (2008).

[21] Emanuel, K. The dependence of hurricane intensity on climate. *Nature*, 326, 2, 483-485 (1987).

[22] Elsner, J. B., J. P. Kossin, and T. H. Jagger (2008), The increasing intensity of the strongest tropical cyclones, *Nature*, 455, 92–95.

[23] Knutson, T. R. et al. Tropical cyclones and climate change. *Nature Geosci.*, 3.3, 157-163 (2010).

[24] Emanuel, K. A. Downscaling CMIP5 climate models shows increased tropical cyclone activity over the 21st century, *Proc. Natl. Acad. Sci.*, 110(30), 12,219–12,224, (2013).

[25] Luettich R.A., Westerink, J.J. & Scheffner, N.W. ADCIRC: *An Advanced Three-dimensional Circulation Model for Shelves, Coasts and Estuaries, Report 1: Theory and Methodology of ADCIRC-2DDI and ADCIRC-3DL*. DRP Technical Report DRP-92-6. (Department of the Army, US Army Corps of Engineers, Waterways Experiment Station, Vicksburg, MS, 1992).

[26] Lin, N., P. Lane, K. A. Emanuel, R. M. Sullivan, and J. P. Donnelly. Heightened hurricane surge risk in northwest Florida revealed from climatological-hydrodynamic modeling and paleorecord reconstruction, *J. Geophys. Res. Atmos.*, 119, doi:10.1002/2014JD021584, (2014).

[27] Aerts, J. C. J. H., Lin, N., Botzen, W., Emanuel, K. & de Moel, H. Low-Probability Flood Risk Modeling for New York City. *Risk Analysis* 33, 772–788 (2013).

[28] Aerts, J. C. J. H. et al. Evaluating Flood Resilience Strategies for Coastal Megacities. *Science* 344, 473–475 (2014).

[29] Weisberg, R. H. & Zheng, L. Hurricane storm surge simulations for Tampa Bay. *Estuaries and Coasts: J ERF* 29, 899–913 (2008).

[30] Kalnay, E. et al. The NCEP/NCAR 40-year reanalysis project. *Bull. Amer. Meteor. Soc.*, **77**, 437-471 (1996).

[31] Bossak, B. H. *Early 19th century US hurricanes: a GIS tool and climate analysis*. Ph.D. Dissertation, Florida State University (2003).

[32] Morey, S. L., Baig, S., Bourassa, M. A., Dukhovskoy, D. S. & O'Brien, J. J. Remote forcing contribution to storm-induced sea level rise during Hurricane Dennis. *Geophys. Res. Lett.* 33, L19603 (2006).

[33] Chavas, D. R. & Emanuel, K. A. A QuikSCAT climatology of tropical cyclone size. Geophys. Res. Lett. 37.18 (2010).

[34] Rotunno, R., and K.A. Emanuel, 1987: An air-sea interaction theory for tropical cyclones, Part II: Evolutionary study using axisymmetric nonhydrostatic numerical model. J. Atmos. Sci., 44, 542-561.

[35] Chavas, D. R. and K. Emanuel. Equilibrium Tropical Cyclone Size in an Idealized State of Axisymmetric Radiative–Convective Equilibrium*. *J. Atmos. Sci.*, 71, 1663–1680. (2014). doi: http://dx.doi.org/10.1175/JAS-D-13-0155.1

[36] Emanuel, K. A. An air-sea interaction theory for tropical cyclones. Part I: Stady-state maintenance. *J. Atmos. Sci.,* 43, 585-605 (1986).

[37] Nott, J., Green, C., Townsend, I. & Callaghan, J. The World Record Storm Surge and the Most Intense Southern Hemisphere Tropical Cyclone: New Evidence and Modeling. *Bull. Am. Meteorol. Soc* 95, 757–765 (2014).

[38] Hardy T, L. Mason, and A. Astorquia (2004), Surge plus tide statistics for selected open coast locations along the Queensland east coast. Queensland Climate Change and Community Vulnerability to Tropical Cyclones. Ocean Hazards Assessment Stage 3. Queensland Government Report, July 2004.

[39] Haigh, I. D. et al. Estimating present day extreme water level exceedance probabilities around the coastline of Australia: tropical cyclone-induced storm surges. *Clim Dyn* 42, 139–157 (2014).

[40] Nott, J. F. & Jagger, T. H. Deriving robust return periods for tropical cyclone inundations from sediments. *Geophys. Res. Lett.* (2012). doi:10.1029/2012GL054455

[41] Evan, A. T. & Camargo, S. J. A climatology of Arabian Sea cyclonic storms. *J. Climate* (2011). doi:10.1175/2010JCLI3611.1

[42] Rienecker, M.M., M.J. Suarez, R. Gelaro, R. Todling, J. Bacmeister, E. Liu, M.G. Bosilovich, S.D. Schubert, L. Takacs, G.-K. Kim, S. Bloom, J. Chen, D. Collins, A. Conaty, A. da Silva, et al.

(2011), MERRA: NASA's Modern-Era Retrospective Analysis for Research and Applications. *J. Climate*, 24, 3624-3648, doi:10.1175/JCLI-D-11-00015.1.

[43] Shirvani, A., Nazemosadat, S. M. J. & Kahya, E. Analyses of the Persian Gulf sea surface temperature: prediction and detection of climate change signals. *Arab J Geosci*, 8:2121–2130, (2015).

[44] Evan, A. T., Kossin, J. P., Eddy' Chung, C. & Ramanathan, V. Arabian Sea tropical cyclones intensified by emissions of black carbon and other aerosols. *Nature* 479, 94–97 (2011).

[45] Woodruff, J. D., Irish, J. L. & Camargo, S. J. Coastal flooding by tropical cyclones and sea-level rise. *Nature* 504, 44–52 (2013).

Author contributions K. E. performed numerical simulations of the storms. N. L carried out storm surge simulations and statistical analysis. N.L. and K.E. co-wrote the paper.

Additional information The authors declare no competing financial interests. Methods and Supplementary Information accompany this paper on www.nature.com/naturegeoscience.

Correspondence and requests for materials should be addressed to N.L. (nlin@princeton.edu).

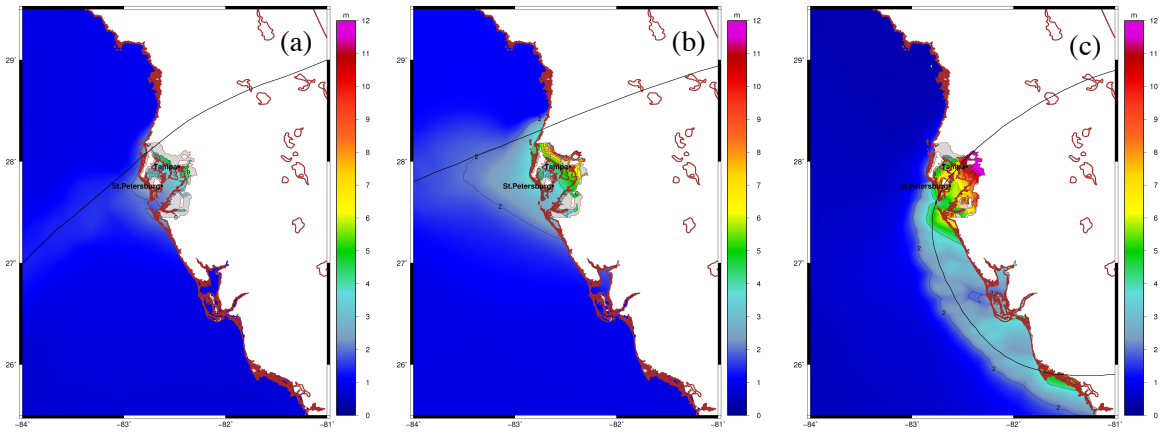

Figure 1. Two grey swan TCs (b and c) for Tampa compared to the 1921 Tampa Hurricane (a). The shaded contours represent the simulated surge height (m; above MSL); the maximum surge at Tampa (82.45W, 27.94N) is 4.0 m, 5.9 m, and 11.1 m for (a)-(c), respectively. The black curve shows the storm track. The storm characteristics when the storm moves closest to Tampa Bay mouth (82.72W, 27.58N) are (a). storm symmetrical maximum wind speed V_m = 43.1 m/s, minimum sea-level pressure P_c = 967.8 mb, radius of maximum wind R_m = 35.0 km, distance to the Bay mouth ds = 37.7 km, translation speed U_t = 4.6 m/s, and translation direction θ_t = 51.8 deg; (b). V_m = 54.7 m/s, P_c = 953.4 mb, R_m = 39.7 km, ds = 75.0 km, U_t = 5.6 m/s, and θ_t = 67.6 deg; and (c). V_m = 104.3 m/s, P_c = 829.6 mb, R_m = 17.0 km, ds = 5.1 km, U_t = 2.0 m/s, and θ_t = 20.0 deg.

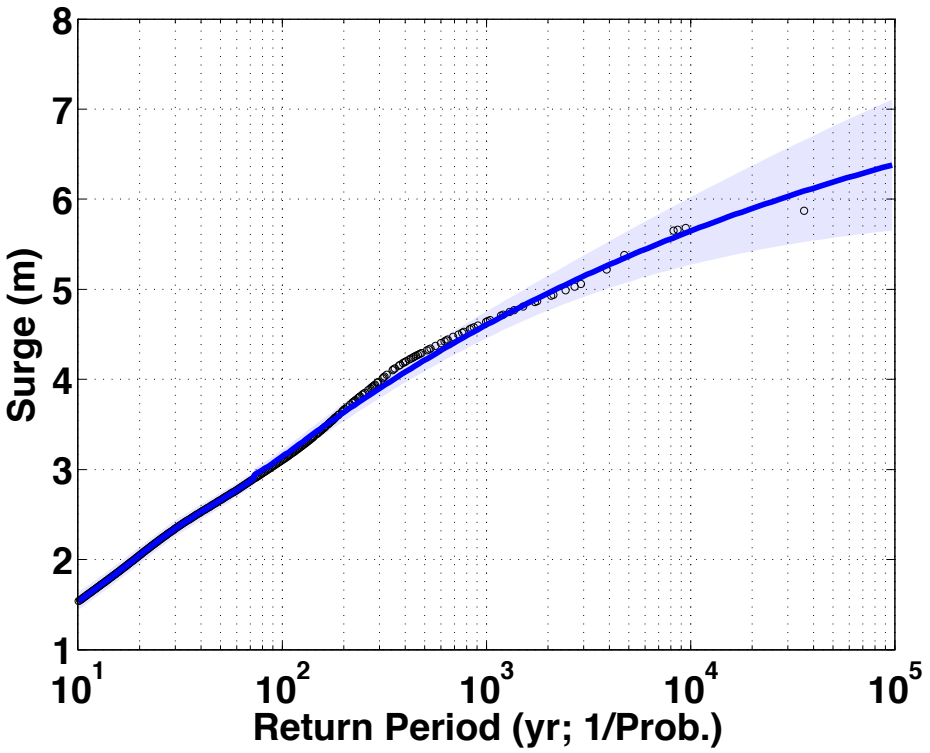

Figure 2. Estimated storm surge level as a function of the return period for Tampa (82.45W, 27.94N) for the NCEP/NCAR reanalysis climate of 1980-2005, based on 7800 synthetic events. The associated annual frequency of the synthetic events is 0.36. Black dots show the simulated data, and the shade shows the 90% statistical confidence interval.

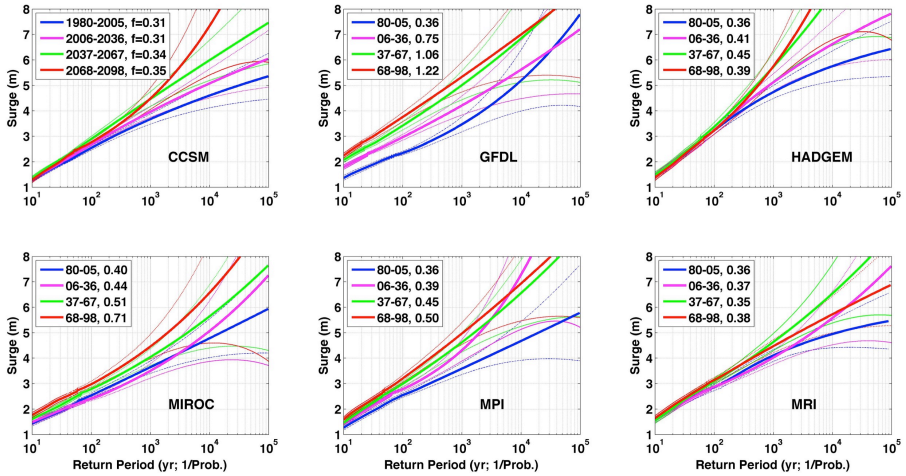

Figure 3. Estimated storm surge level as a function of the return period for Tampa (82.45W, 27.94N) in the climate of 1980-2005 (blue), 2006-2036 (pink), 2037-2067 (green), and 2068-2098 (red), projected using each of 6 the climate models for the IPCC AR5 RCP8.5 emission scenario. The annual frequency (f) is noted for each case. The thin dash curves show the 90% statistical confidence interval. (The data points and goodness of fit for the upper tail are shown in Supplementary Fig. S1.)

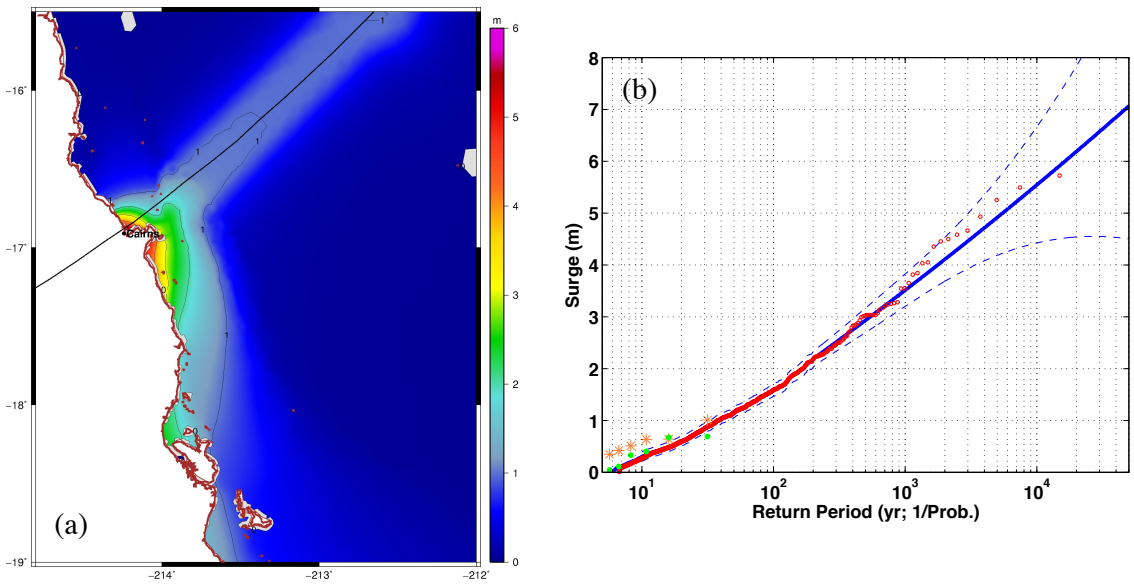

Figure 4. Storm surge risk analysis for Cairns, based on 2400 synthetic events in the NCEP/NCAR reanalysis climate of 1980-2010. The associated annual frequency for the synthetic events is 0.16. (a). The "worst" surge event for Cairns (145.76E, 16.91S). The shaded contours show the simulated surge height (m; above MSL). The black curve shows the storm track. The storm characteristics when the storm moves closest to Cairns are V_m = 79.3 m/s, P_c = 901.1 mb, R_m = 22.3 km, ds = 9.9 km, U_t = 6.2 m/s, and θ_t = 234.4 deg. (b). Estimated storm surge level as a function of the mean return period for Cairns. The red dots show the synthetic data, and the dash curves show the 90% statistical confidence interval. Orange dots show the tidal-gauge-observed Cairns storm surges (6 in total) between 1980-2010; green dots show the simulated surges for these 6 historical TCs (the annual frequency of the historical storms is 0.19).

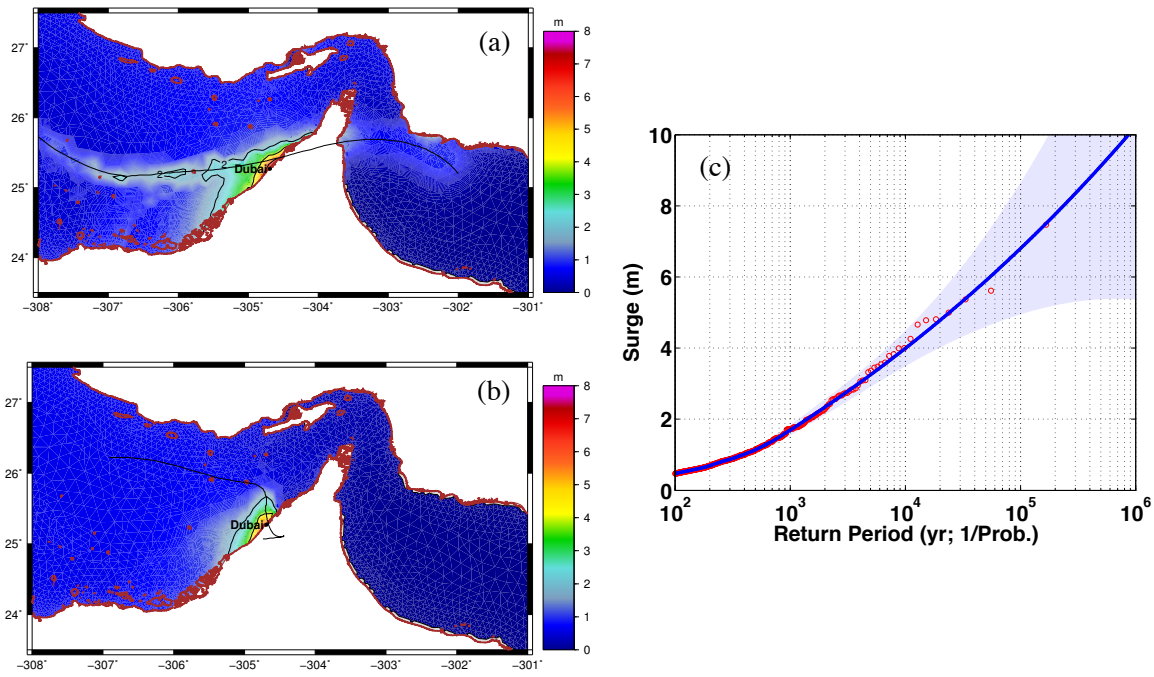

Figure 5. Storm surge risk analysis for Dubai, based on 3100 synthetic events in the MERRA reanalysis climate of 1980-2010. The associated annual frequency for the synthetic events is 0.037. (a). The "worst" surge (7.5 m) event for Dubai (55.31E, 25.27N). The shaded contours show the simulated surge height (m; above MSL). The black curve shows the storm track. The storm characteristics when the storm moves closest to Dubai are V_m = 114.6 m/s, P_c = 784.2 mb, R_m = 13.8 km, ds = 18.4 km, U_t = 3.0 m/s, and θ_t = 77.0 deg. (b). The second "worst" surge (5.6 m) event for Dubai, with V_m = 65.4 m/s, P_c = 927.3 mb, R_m = 21.3 km, ds = 7.8 km, U_t = 0.7 m/s, and θ_t = 159.5 deg. (c). Estimated storm surge level as a function of the return period for Dubai. The dots show the synthetic data, and the shade shows the 90% statistical confidence interval.

Methods

Grey Swan Tropical Cyclones

Ning Lin[1*] and Kerry Emanuel[2]

[1]Department of Civil and Environmental Engineering, Princeton University, Princeton, NJ 08544, USA

[2]Department of Earth, Atmospheric, and Planetary Sciences, Massachusetts Institute of Technology, Cambridge, MA 02139-4307, USA

[*]Corresponding author, nlin@princeton.edu

Methods

Storm generation

The climatological-hydrodynamic method includes three components: storm generation, storm surge simulation, and statistical analysis. We use a statistical-deterministic TC model[19] to generate enough synthetic TCs in an ocean basin under a given climate to obtain a desired number of TCs that make landfall in a particular coastal area of interest. Weak proto-storms are seeded uniformly over the basin within a large-scale environment provided by a reanalysis or climate model data set. Once initialized, the storms move in accordance with the large-scale environmental wind. Along each storm track, the Coupled Hurricane Intensity Prediction System[46] (CHIPS), a dynamic model, is used to simulate the storm intensity according to environmental conditions such as potential intensity, wind shear, humidity, and the thermal stratification of the ocean. These environmental conditions are modeled statistically based on the reanalysis or climate model data set. The CHIPS model also predicts the storm radius of maximum wind (R_m), given an externally supplied storm outer radius (R_o). We apply the observed basin mean of R_o based on the historical record (e.g., 400 km for North Atlantic storms[33]) and assume it is constant over the lifecycle of a storm[33]. Then we estimate R_m (varying from storm to storm and over the lifecycle of a storm) from CHIPS.

We design specific criteria (a filter) for each study area to select local storms from basin-wide events. Various storm tracks can induce significant surges in Tampa Bay, including those that make landfall within or near the Bay as well as those that travel close offshore and parallel to the coast. To capture all these storms, we create a two-line-segment filter encompassing the Bay and surrounding coastal region. One line segment links a point on the coast (82.81W,

29.17N), about 180 km north of the Bay's mouth, to a point over the ocean (83.8W, 27.58N) about 100 km west of the Bay's mouth. The other line segment links the ocean point (83.8W, 27.58N) to a coastal point (82.407W, 27.0N) about 70 km south of the Bay's mouth. We select all storms that cross either of these two line segments with intensity greater than 21 m/s; we call these storms "Tampa Bay storms." Simpler, circular filters are created for the other study areas. We create a circle centered in Cairns (145.76E, 16.91S) with a radius of 100 km to select all "Cairns storms" that move into this circle with intensity great than 21 m/s. Similarly, we create 100-km-radius circular filters centered at Dubai (55.31E, 25.27N), Abu Dhabi (54.37E, 24.47N), and Doha (51.53E, 25.28N).

Given the storm characteristics of selected storms in a study area, we estimate the surface wind and pressure fields using parametric methods fit to the explicitly modeled maximum wind speed, radius of maximum winds, and minimum surface pressure. In particular, the surface wind (10-min wind at 10 m) is estimated by fitting the wind velocity at the gradient height to an analytical hurricane wind profile[47], translating the gradient wind to the surface level with a velocity reduction factor (0.85) and an empirical formula for inflow angles, and adding a fraction (0.55 at 20 degrees cyclonically) of the storm translation velocity to account for the asymmetry of the wind field induced by the surface background wind[48]. The surface pressure is estimated also from a simple parametric model[49].

Surge simulation

With the storm surface wind and pressure fields as input, we apply the Advanced Circulation (ADCIRC) model[25] to simulate the storm surge. ADCIRC is a finite element hydrodynamic

model that has been validated and applied to simulate storm surges and make forecasts for various coastal regions[50,51]. It allows the use of an unstructured grid with very fine resolution near the coast and much coarser resolution in the deep ocean. The ADCIRC mesh we developed for Tampa covers the entire Gulf of Mexico. The mesh has a peak resolution of about 100 m along the west Florida coast near Tampa and extends on land up to the 10-m height contour in the Tampa Bay area. The meshes developed for other study regions are relatively coarser (given coarser bathymetric data). To capture the effect of storms approaching from various directions, the mesh for Cairns has as its lower boundary the Australian coastline of Queensland, the Northern Territory, and part of Western Australia. The mesh extends over the Indian and South Pacific Oceans (from 114.0E to 176.0E) and is bounded above by Indonesia and Indonesian New Guinea. The resolution is about 1 km on the Queensland coast around Cairns. The mesh developed for Dubai covers the entire Persian Gulf and extends over the Arabian Sea (down to 16.0N). The resolution is about 2 km near Dubai. The same mesh is used for Abu Dhabi and Doha; the resolution around these two locations is about 3-4 km.

To evaluate our surge modeling configuration and ADCIRC meshes, we simulated historical events for Tampa and Cairns (the Persian Gulf has no historical storms), with the storm characteristics obtained from the Best Track databases[52,53]. The simulated storm surge in Tampa for the 1921 hurricane is about 4.0 m (see Fig. 1a in the main article), which is comparable to that observed in this region (~3.3-3.8 m, considering the storm tide was estimated to be 3.0-3.5 m and happening likely at low tide), given the large uncertainties in both the observed surge level and storm characteristics (especially the size) for this early storm. (Note that in this case, because an observation of R_m is available only at landfall and there is no information about R_o, we estimated R_o from the landfall R_m using an empirical relationship[26] between them and the

77 wind intensity and then kept the estimated R_o constant to estimate R_m for the time periods before
78 landfall using the empirical relationship.) For Cairns, we simulated storm surges for all 6
79 historical Cairns storms between 1980-2010 (selected using the same filter as for the synthetic
80 storms) plus Cyclone Yasi in 2011. Simulations are close to the observations for the most
81 significant events, including Cyclones Justin (1997), Rona (1999), and Yasi (see Supplementary
82 Fig. S4), but the simulation underestimates the surge for Cyclone Steve (2000). Not all simulated
83 historical surges match well with the observations individually, mainly due to the uncertainty in
84 storm size (since an empirical estimate[26] of the R_m using the basin mean R_o was applied due to the
85 lack of observations). However, the simulations compare relatively well with all observations
86 statistically (see Fig. 4 in the main article).

87

88 *Statistical analysis*

89 Statistical analysis is performed on the synthetic surge datasets. For a specific location and a
90 given climate scenario, we assume the arrival of storms to be a stationary Poisson process, with
91 arrival rate as the storm annual frequency. For each storm arrival, the probability density
92 function (PDF) of its induced storm surge is characterized by a long tail. We apply a Peaks-
93 Over-Threshold (POT) method to model this tail with a Generalized Pareto Distribution (GPD),
94 using the maximum likelihood method, and the rest of the distribution with non-parametric
95 density estimation. The estimated storm annual frequency and surge PDF are then combined to
96 calculate the (mean) return period (the reciprocal of the annual exceedance probability) for
97 various surge levels[13], with the associated statistical confidence interval calculated using the
98 Delta method[54].

99 **Additional References**

[46] Emanuel, K., C. Des Autels, C. Holloway, and R. Korty. Environmental control of tropical cyclone intensity, *J. Atmos. Sci.,* 61, 843–858, doi:10.1175/1520-0469(2004)061<0843:ECOTCI>2.0.CO;2, (2004).

[47] Emanuel, K. & Rotunno, R. Self-Stratification of Tropical Cyclone Outflow. Part I: Implications for Storm Structure. *J. Atmos. Sci.* 68, 2236–2249 (2011).

[48] Lin, N. & Chavas, D. On hurricane parametric wind and applications in storm surge modeling. *J. Geophys. Res.* 117, D09120 (2012).

[49] Holland, G.J. An analytic model of the wind and pressure profiles in hurricanes. *Mon. Weather Rev.*, 108, 1212-1218 (1980).

[50] Westerink, J. J., et al. A basin- to channel-scale unstructured grid hurricane storm surge model applied to southern Louisiana. *Mon. Weather Rev.*, 136, 833-864 (2008). doi:10.1175/2007MWR1946.1

[51] Dietrich J.C. et al. Modeling hurricane waves and storm surge using integrally-coupled, scalable computations. *Coast. Eng.*, 58, 1, 45-65 (2011).

[52] Landsea, C. W., S. Feuer, A. Hagen, D. A. Glenn, J. Sims, R. Perez, M. Chenoweth, and N. Anderson: A reanalysis of the 1921-1930 Atlantic hurricane database. *Journal of Climate*, 25, 865-885, 2012.

[53] Knapp, K. R., Kruk, M. C., Levinson, D. H., Diamond, H. J., & Neumann, C. J. The international best track archive for climate stewardship (IBTrACS) unifying tropical cyclone data. *Bulletin of the American Meteorological Society*, 91(3), 363-376 (2010).

[54] Coles, S. *An Introduction to Statistical Modeling of Extreme Values*. (Springer, London, 2001).

Supplementary Information

Grey Swan Tropical Cyclones

Ning Lin[1*] and Kerry Emanuel[2]

[1]Department of Civil and Environmental Engineering, Princeton University, Princeton, NJ 08544, USA

[2]Department of Earth, Atmospheric, and Planetary Sciences, Massachusetts Institute of Technology, Cambridge, MA 02139-4307, USA

[*]Corresponding author, nlin@princeton.edu

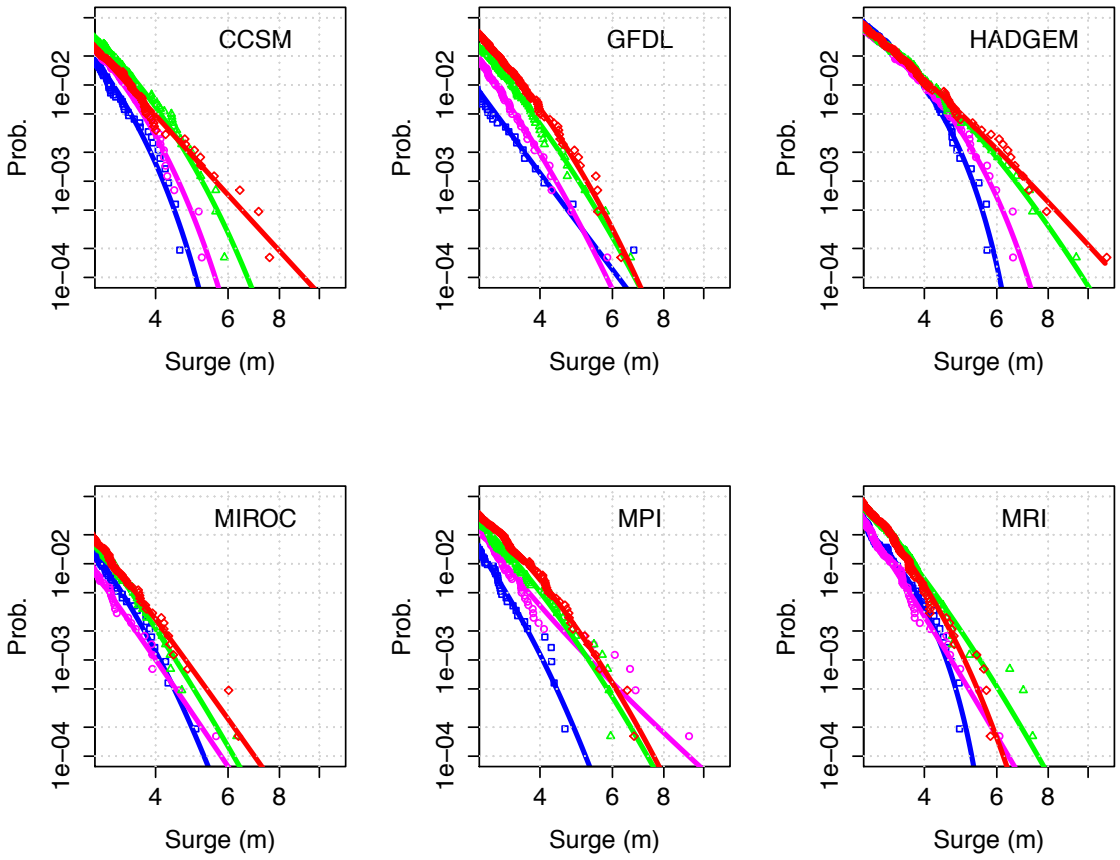

Figure S1. Generalized Pareto distribution (GPD) fit (curves) of the upper tail of the distribution (dots) of storm surge for Tampa, in the climate of 1980-2005 (blue), 2006-2036 (pink), 2037-2067 (green), and 2068-2098 (red), projected using each of the 6 climate models for the IPCC AR5 RCP8.5 emission scenario.

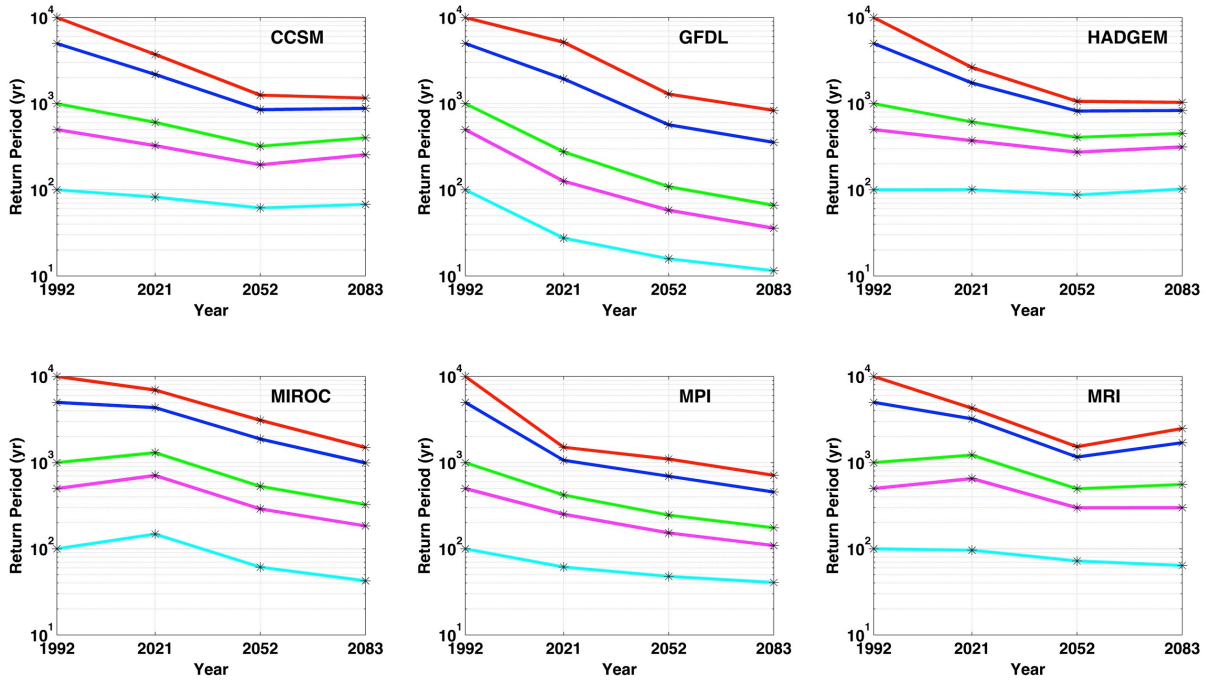

Figure S2. The change of the return period of a 10,000-year (red), 5,000-year (blue), 1,000-year (green), 500-year (pink), and 100-year (cyan) event from the late 20th century to the late 21st century, projected for Tampa, using each of the 6 climate models for the IPCC AR5 RCP8.5 emission scenario. Black stars show the estimated return periods for the climates of 1980-2005 (control), 2006-2036 (early 21st century), 2037-2067 (middle), and 2068-2098 (late), marked at the center years of 1992, 2021, 2052, and 2083, respectively. These estimates are consistent with those in Fig. 3 of the main article. Linear interpolation is applied between the marked points in this figure.

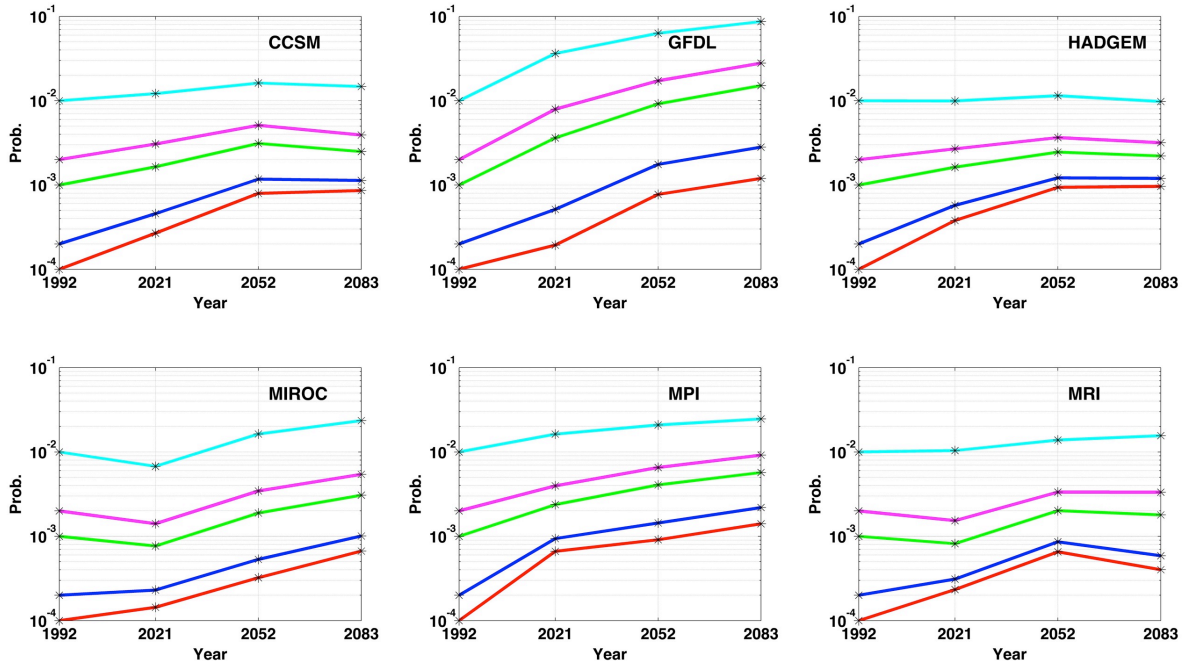

Figure S3. Same as Fig. S2, but presented as the change of annual exceedance probability (the reciprocal of the mean return period).

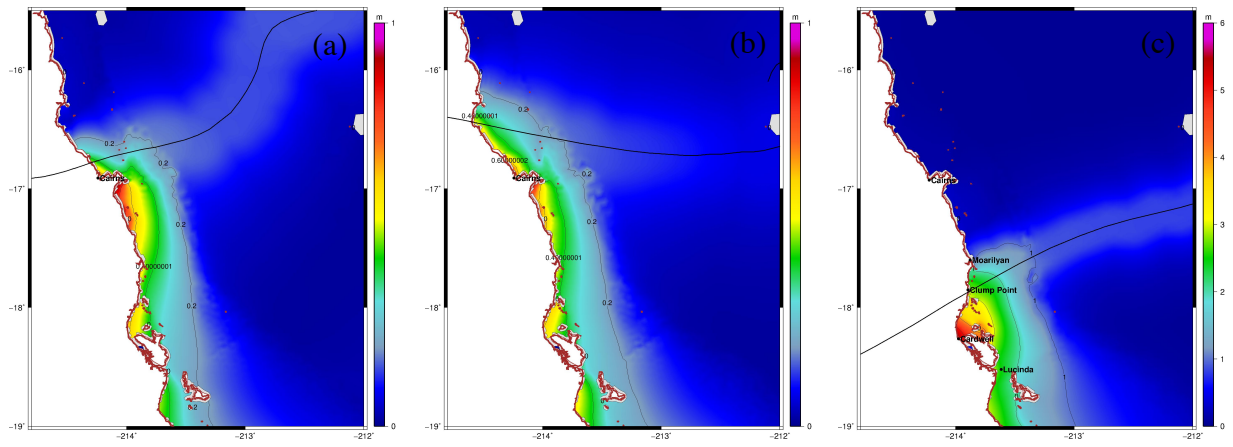

Figure S4. Simulated surges for three historical storms in the Cairns region. (a). Cyclone Justin of 1997. The simulated surge at Cairns is 0.69 m (the observation is 0.63 m). (b). Cyclone Rona of 1999. The simulated surge at Cairns is 0.67 (the observation is 0.63 m). (c). Cyclone Yasi of 2011. The simulated surges at Moarilyan, Clump Point, Cardwell, and Lucinda are 1.03 m, 2.88 m, 5.45 m, and 2.48 m, respectively (the observations are 1.30, 2.97, 5.33, and N/A due to tidal gauge failure). The shaded contours show the simulated surge height (m; above MSL). The black curve shows the storm track. (The observed storm surge is estimated as the difference between the observed maximum water level, obtained from the State of Queensland, Department of Science, Information Technology, Innovation and the Arts, and the predicted astronomical tide, obtained from the Australian National Tidal Center.)

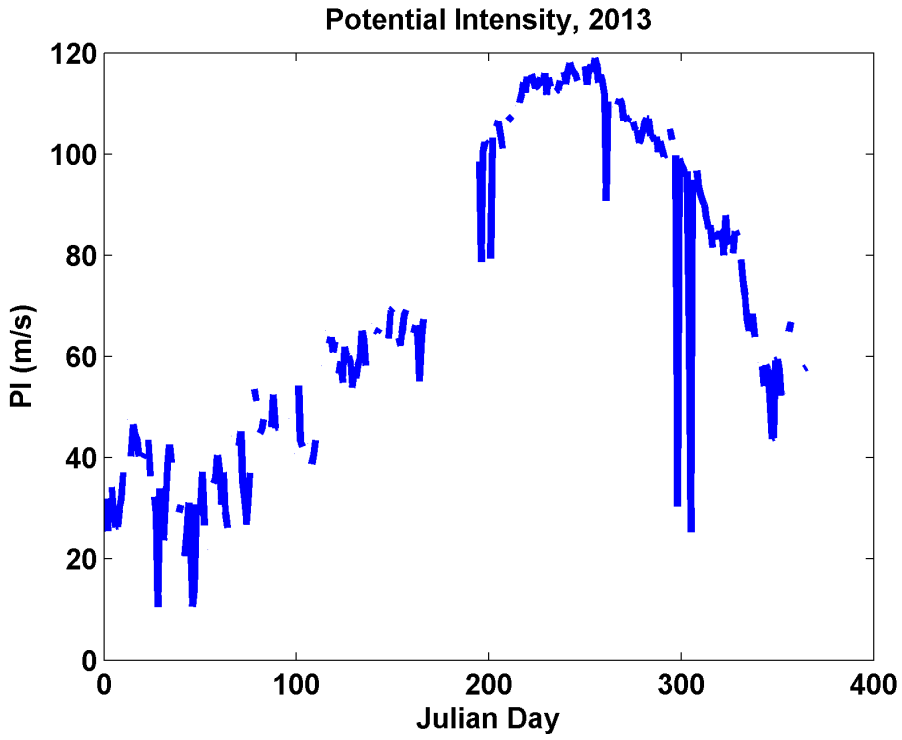

Figure S5. Daily potential intensity (PI) in the Persian Gulf during the year 2013. Data applied in the calculation includes the atmospheric sounding at Dammam, Saudi Arabia, for 12 GMT each day (data obtained from the University of Wyoming atmospheric data website) and monthly mean Hadley Center SSTs averaged over the whole Persian Gulf and linearly interpolated to the day. The blank sections represent days with missing soundings.

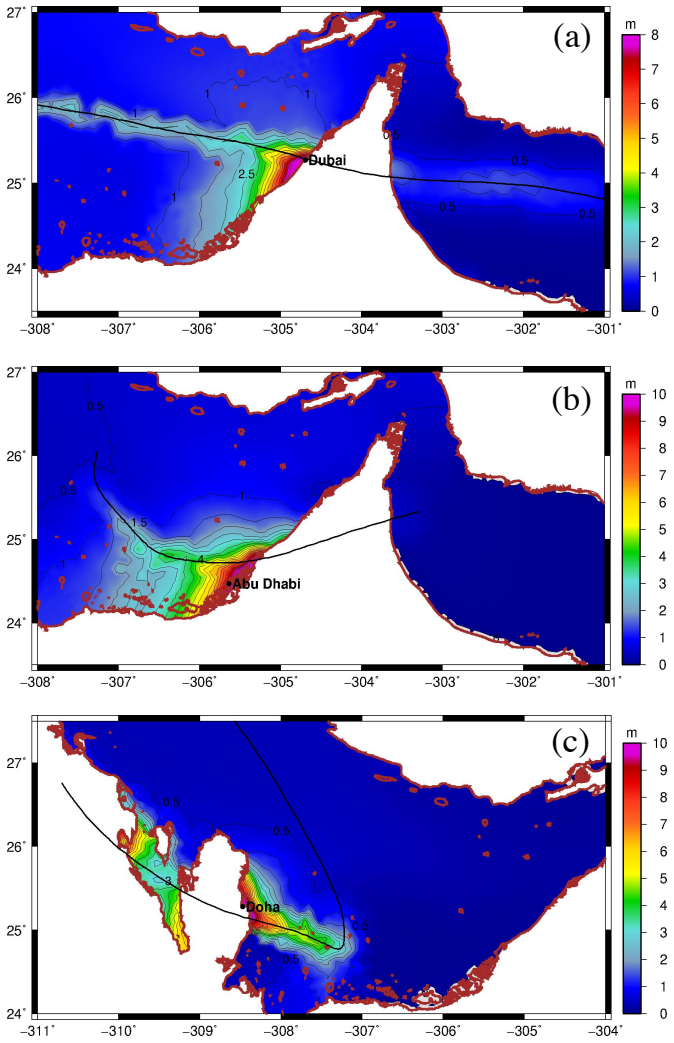

Figure S6. Three grey swan TC surge events for three major cities in the Persian Gulf, based on the NCEP/NCAR reanalysis climate of 1980-2010. (a). The worst surge event (among 3100 events), inducing a maximum surge of 7.1 m for Dubai. (b). The worst surge event (among 3100 events), inducing a maximum surge of 9.5 m for Abu Dhabi. (c). The worst surge event (among 3100 events), inducing a maximum surge of 9.1 m for Doha. (The higher surges in Abu Dhabi and Doha compared to Dubai are mainly induced by their different local geophysical features; the lower resolutions in the numerical mesh may have also led to overestimates; see Methods.)

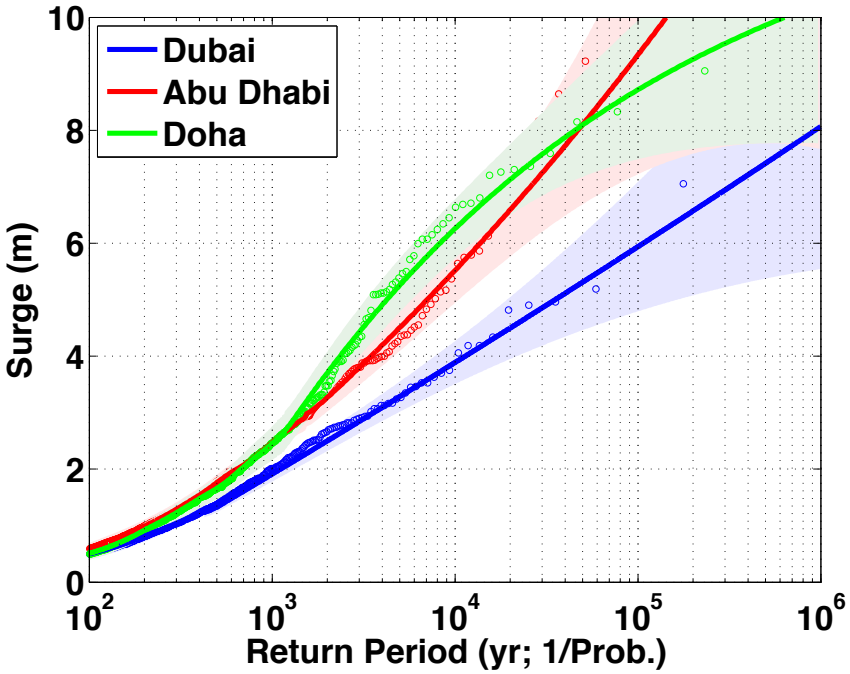

Figure S7. Estimated storm surge level as a function of return period for Dubai (blue), Abu Dhabi (red), and Doha (green), each based on 3100 synthetic events in the NCEP/NCAR reanalysis climate of 1980-2010. The associated annual frequencies of the synthetic events are 0.032, 0.024, and 0.025 for Dubai, Abu Dhabi, and Doha, respectively. The dots show the synthetic data, and the shading shows the 90% statistical confidence interval. (The return level curve for Dubai is very similar to that obtained based on the MERRA reanalysis, as shown in Fig. 5c in the main article.)